Crossover from Two- to Three-Dimensional Contraction of Polymer Chains in Semidilute Solutions Confined to a Narrow Slit

Iwao Teraoka*

Herman F. Mark Polymer Research Institute, Polytechnic University, Six MetroTech Center, Brooklyn, New York 11201

Yongmei Wang

Department of Chemistry, North Carolina A & T State University, Greensboro, North Carolina 27411

Received April 11, 2000
Revised Manuscript Received June 26, 2000

Introduction

Chains with excluded-volume interactions are swollen at low concentrations. The swelling depends on the dimensions D of the space allowed for the chains. The linear dimension of the chain consisting of N monomers scales as $N^{3/(D+2)}$.[1] Polymer chains confined to a slit between two parallel plates have characteristics between those of two-dimensional (2D) and three-dimensional (3D) chains.[2] Confinement by a narrow slit extends the chains along the slit walls, and the overall shape resembles a pancake. An increasing confinement strength R_{g0}/d flattens the pancake, where R_{g0} is the radius of gyration of the isolated chain in the 3D solution and d is the slit width. In the narrow slit limit, the chain conformation should be identical to that of the 2D chains.

In the semidilute solution, shielding of the excluded-volume effect contracts the chains, and the overall chain conformation becomes that of an ideal chain. The linear dimension of the ideal chain scales as $N^{1/2}$ in all dimensions. Thus, the contraction effect is more significant in the 2D chains compared with the 3D chains. In a slit of a finite width, the contraction characteristics will be between those of 2D and 3D solutions,[2] depending on R_{g0}/d. Weakly confined chains contract as the 3D chains do. Contraction of strongly confined chains will be 2D-like, but it decreases the confinement strength simultaneously. Therefore, the contraction characteristics will exhibit a crossover from 2D to 3D as the correlation length ξ decreases. Daoud and de Gennes[2] used the scaling theory to predict that the crossover depends on ξ/d. Computer simulations that examined the chain contraction in 2D[3] or in the confined solutions[4−6] are limited, however.

Earlier we performed Monte Carlo simulations for self-avoiding random walks on a cubic lattice and examined the radius of gyration R_g at different volume fractions ϕ of the chains.[6] The contraction factor $r_{3D} \equiv R_g/R_{g0}$ obtained for chains of different lengths was on a master curve given by the semiempirical formula

$$r_{3D} = [1 + 0.96403(\phi/\phi^*) + 0.34890(\phi/\phi^*)^2]^{-1/16} \quad (1)$$

where ϕ^* is the overlap concentration estimated from $(\phi^*/N)[2^{1/2}(R_{g0}/a + 0.199)]^3 = 1$ with a being the lattice spacing.

Here we use our simulation results to examine the contraction characteristics for chains confined to a slit. After studying the contraction of 2D chains, we compare the contraction in chains of different lengths confined to slits of different widths to uncover universal crossover characteristics. Simulations were performed by generating self-avoiding random walks of $N - 1$ steps, where $N = 100$, 200, 400, and 800, in a simulation box that consists of a given number of layers extending in x and y directions in a cubic lattice. The two layers adjacent to the box represent the slit walls. The slit width d is given by $d/a = 1 +$ (the number of the layers in the box). A periodic boundary condition was applied to the x and y directions. Chains were moved by the reptation mechanism until equilibrium was reached. Simulations for the 2D chains were performed on a square lattice. Some of the results presented here were reported in our preceding contribution.[6] In the latter, our attention was on the isotropic average of the chain dimensions and the structure factors, and we were short on elucidating the 2D and 3D characteristics of the contraction.

2D Chains

In this section only, R_g and R_{g0} are the radius of gyration of a 2D chain and its dilute-solution value, and ϕ and ϕ * are the area fraction of the chains and its value at the chain overlap. We first review the scaling theory for chain molecules consisting of N monomers ($N \gg 1$) placed on a square lattice of spacing a.[7] In the dilute solution limit, R_{g0} is given as

$$R_{g0} \cong aN^{3/4} \quad (2)$$

The overlap concentration ϕ^* is given as

$$\phi^* \cong Na^2R_{g0}^{-2} \cong N^{-1/2} \quad (3)$$

At $\phi \gg \phi^*$, the solution of the 2D chains is dictated by the correlation length ξ_{2D} over which the monomer density loses its correlation exponentially. The ξ_{2D} is close to R_{g0} at $\phi = \phi^*$ and decreases as ϕ increases. We write $\xi_{2D} \cong R_{g0}(\phi/\phi^*)^m$ with a scaling exponent m. With eqs 2 and 3, we find $\xi_{2D} \cong a\phi^m N^{3/4+m/2}$. The requirement that ξ_{2D} be independent of N leads to $m = -3/2$. Thus,

$$\xi_{2D} \cong a\phi^{-3/2} \quad (4)$$

as opposed to $\xi_{3D} \cong a\phi^{-3/4}$ for the 3D chains.

We can estimate the chain dimension by using a blob picture. Within a blob of size ξ_{2D}, the chain is an excluded-volume 2D chain, but beyond ξ_{2D}, the chain behaves ideally. Let g be the number of monomers in the blob. Then, $\xi_{2D} \cong ag^{3/4}$. The whole chain can be regarded as an ideal chain of N/g blobs of size ξ_{2D}. Therefore, $R_g \cong \xi_{2D}(N/g)^{1/2} \cong aN^{1/2}\phi^{-1/2}$, which leads to

$$R_g/R_{g0} \cong N^{-1/4}\phi^{-1/2} \cong (\phi/\phi^*)^{-1/2} \quad (5)$$

The exponent to ϕ/ϕ^* is $-1/8$ for the 3D chains. Combining eqs 2−4, we have $\xi_{2D}/R_{g0} \cong (\phi/\phi^*)^{-3/2}$. Together with eq 5,

$$\xi_{2D}/R_{g0} \cong (R_g/R_{g0})^3 \quad (6)$$

Now we present our simulation results for the 2D chains. Table 1 lists R_{g0} and ϕ^* for the chains with $N =$

10.1021/ma0006373 CCC: $19.00 © 2000 American Chemical Society
Published on Web 08/18/2000

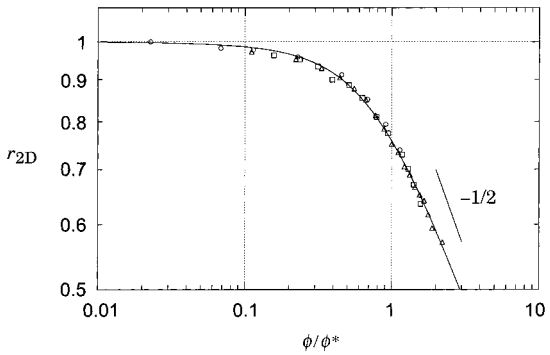

Figure 1. Contraction factor $r_{2D} = R_g/R_{g0}$ of 2D chains (N = 100 (circles), 200 (squares), and 400 (triangles)), plotted as a function of ϕ/ϕ^*. The line is the best fit by the interpolation formula.

Table 1. Characteristics of Two-Dimensional Chains

N	R_{g0}/a	ϕ^*
100	10.491	0.4389
200	17.782	0.3099
400	29.979	0.2199

100, 200, and 400 used in the simulations. The ϕ^* was calculated according to

$$\phi^*[2^{1/2}(R_{g0}/a + 0.1825)]^2 = N \quad (7)$$

As in 3D, discreteness of the simulation space must be considered to use the equations derived for a continuous space. Two monomers separated by a (center-to-center) are in close contact. The correction of 0.1825 is equal to a half of $R_{g0}/R_0 = (0.799/6)^{1/2}$, where R_0^2 is the mean-square end-to-end distance.[7]

Figure 1 shows the contraction factor $r_{2D} = R_g/R_{g0}$ as a function of ϕ/ϕ^*. The data obtained for different lengths appear to be on a master curve approximated by

$$r_{2D} \equiv R_g/R_{g0} = [1 + 0.59747(\phi/\phi^*) + 1.3849(\phi/\phi^*)^2]^{-1/4} \quad (8)$$

which agrees with eq 5 at $\phi/\phi^* \gg 1$.

Chains Confined to a Narrow Slit

A sufficiently long chain confined to a narrow slit is modeled by a sequence of blobs of size d. The partial chain within each blob is a 3D excluded-volume chain. The number of monomers in the blob, g, is estimated from $d \cong ag^{3/5}$. We look at $R_{g||}$, the root-mean-square of the x and y components in R_g^2. In the dilute solution limit, the sequence of blobs is a 2D self-avoiding walk (pancake). Hence, $R_{g0||} \cong d(N/g)^{3/4}$. Together with $R_{g0} \cong aN^{3/5}$ for the 3D chains, we obtain $R_{g0||}/R_{g0} \cong (R_{g0}/d)^{1/4}$ for chains with $R_{g0} \gg d$. When $R_{g0} \ll d$, there is little confinement effect, and the conformation is isotropic, i.e., $R_{g0||}/R_{g0} = (2/3)^{1/2}$. Figure 2 shows a plot of $R_{g0||}/R_{g0}$ obtained in the simulations for three different slit widths, d/a = 5, 9, and 19, as a function of R_{g0}/d. The solid line is the best fit by the interpolation formula:

$$R_{g0||}/R_{g0} = [(2/3)^3 + 0.54999(R_{g0}/d)^{3/2}]^{1/6} \quad (9)$$

Now we examine how $R_{g||}$ decreases as ϕ increases. See ref 6 for the three-dimensional characteristics of the chains used. Symbols in Figure 3 show $R_{g||}^2/R_{g0||}^2$ as a function of ϕ for (a) N = 100, d/a = 19; (b) N = 200, d/a = 9; and (c) N = 400, d/a = 5. Also plotted are r_{3D}^2 (solid lines) and r_{2D}^2 (dashed lines). Note that r_{3D} applies also to the lateral component. For r_{2D}^2 we need the 2D overlap concentration ϕ^*_{2D} in a slit of a finite width (overlap of pancakes) in place of the overlap concentration for 2D chains. We estimate ϕ^*_{2D} according to

$$\phi^*_{2D}[2^{1/2}(R_{g0||}/a + 0.1825)]^2[(d/a - 1) \times \min(2R_{g0\perp}/R^\circ_{g\perp}, 1)] = N \quad (10)$$

where $(R_{g0\perp})^2$ is the mean square of the z component in R_g^2 in the dilute solution limit, and $R^\circ_{g\perp}/a = [((d/a - 1)^2 - 1)/12]^{1/2}$ is the value of $R_{g0\perp}$ when the monomers pack $d/a - 1$ layers in the simulation box without voids.

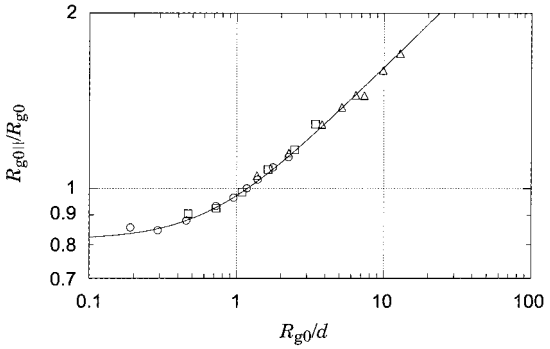

Figure 2. Chain elongation along the slit walls, $R_{g0||}/R_{g0}$, by an increasing confinement strength R_{g0}/d. Symbols are for the slits of width d = 5 (triangles), 9 (squares), and 19 (circles). The line is the best fit by the interpolation formula.

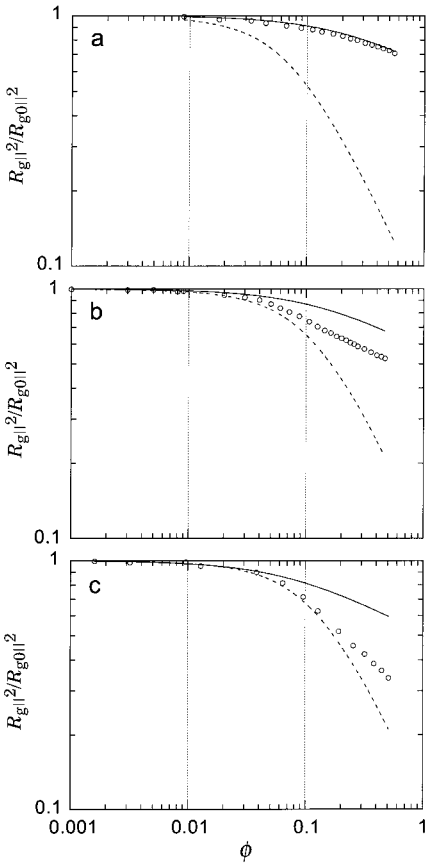

Figure 3. $R_{g||}^2/R_{g0||}^2$ plotted as a function of the polymer volume fraction ϕ. The solid line and the dashed line represent r_{3D}^2 and r_{2D}^2, respectively. (a) N = 100, d = 19, (b) N = 200, d = 9, (c) N = 400, d = 5.

Use of $(d - a) \times \min(2R_{g0\perp}/R°_{g\perp},1)$ for the transverse dimension of the chain is based on the following consideration. When $R_{g0\perp} \ll R°_{g\perp}$, the pancakes can stack on top of the other to occupy the space between the walls. As $R_{g0\perp}$ increases, the number of such pancakes decreases. As $R_{g0\perp}$ exceeds $R°_{g\perp}/2$, the slit can no longer accommodate more than one pancakes at the same position on the slit walls. The pancakes have to be arranged laterally to tessellate the slit. Therefore, the dimension is equal to $d - a$ when $2R_{g0\perp}/R°_{g\perp} > 1$. Otherwise, the dimension is smaller than $d - a$ and proportional to $R_{g0\perp}$.

When the confinement is weak as in Figure 3a, the contraction is close to the 3D line over the entire ϕ. In the strong confinement (c), in contrast, the contraction is close to the 2D line at low ϕ but deviates from the line as ϕ increases. In the intermediate confinement strength (b), the symbols are close to the 2D line at low ϕ and approach the 3D line as ϕ increases. We introduce a parameter α defined by

$$\alpha \equiv \frac{R_{g\parallel}{}^2/R_{g0\parallel}{}^2 - r_{2D}{}^2}{r_{3D}{}^2 - r_{2D}{}^2} \qquad (11)$$

The value of α can vary between 0 (2D-like) and 1 (3D-like). In the Daoud−de Gennes prediction,[2] α depends on the ratio of the 2D correlation length ξ_{2D} to d. The latter can be estimated from eq 6 as $\xi_{2D}/d \cong (R_{g0\parallel}/d)\cdot(R_{g\parallel}/R_{g0\parallel})^3$. Figure 4 shows α as a function of $(R_{g0\parallel}/d)\cdot(R_{g\parallel}/R_{g0\parallel})^3$. The data points obtained for different chain lengths and slit widths appear to be on a master curve, thereby proving the validity of the prediction. We approximate the curve by

$$\alpha = 1/\{1 + 2.2433[(R_{g0\parallel}/d)(R_{g\parallel}/R_{g0\parallel})^3]^2\} \qquad (12)$$

We also prepared a plot of α as a function of $R_{g\parallel}/d$, but the data points did not lead to a master curve. The way the confined chains contract in the semidilute solution changes from a 2D- to 3D-like pattern as ξ_{2D} becomes shorter than d, when the overall dimension is still much larger than d.

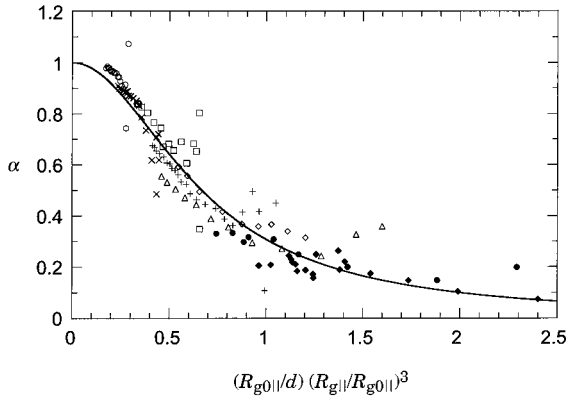

Figure 4. Parameter α plotted as a function of $(R_{g0\parallel}/d)(R_{g\parallel}/R_{g0\parallel})^3$. The chain length and the slit width are 100, 19 (○); 100, 9 (□); 100, 5 (◇); 200, 19 (×); 200, 9 (+); 400, 9 (△); 400, 5 (●); 800, 5 (◆). The solid line represents the best fit by the fitting equation.

Acknowledgment. We appreciate a financial support from NSF (DMR9876360) and PRF (32707-GB5).

References and Notes

(1) de Gennes, P. G. *Scaling Concepts in Polymer Physics*; Cornell University Press: Ithaca, NY, 1979.
(2) Daoud, M.; de Gennes, P. G. *J. Phys. (Paris)* **1977**, *38*, 85.
(3) Carmesin, I.; Kremer, K. *J. Phys. (Paris)* **1990**, *51*, 915.
(4) Milchev, A.; Paul, W.; Binder, K. *Macromol. Theory Simul.* **1994**, *3*, 305.
(5) Pai-Panandiker, R. S.; Dorgan, J. R.; Pakula, T. *Macromolecules* **1997**, *30*, 6348.
(6) Wang, Y.; Teraoka, I. *Macromolecules* **2000**, *33*, 3478.
(7) des Cloizeaux, J.; Jannik, G. *Polymers in Solution: Their Modeling and Structure;* Clarendon: Oxford, 1990.

MA0006373